ELSEVIER

The four-step multiple stage transformation in deformed and annealed Ti$_{49}$Ni$_{51}$ shape memory alloy

P.C. Su, S.K. Wu *

Department of Materials Science and Engineering, National Taiwan University, 1, Roosevelt Rd., Sec. 4, Taipei 106, Taiwan

Abstract

A four-step multiple stage transformation is observed in 20% deformed and 500 °C annealed Ti$_{49}$Ni$_{51}$ shape memory alloy. Two extra B2 → B19′ transformation peaks appear before the previously described B2 → R and R → B19′ peaks while cooling, and these correspond to one new peak, which appears after the original B19′ → B2 peak during heating. These two extra peaks are caused by the combined effect of severe cold-working and long-time annealing on Ti$_{49}$Ni$_{51}$ alloy, and they come separately from the B2 → B19′ transformation occurring in regions with low and high dislocation densities, which are originally suppressed by cold-working.
© 2003 Acta Materialia Inc. Published by Elsevier Ltd. All rights reserved.

1. Introduction

The transformation sequence of TiNi shape memory alloys (SMAs) has been widely investigated in the past decades. In the equiatomic TiNi SMA, the martensitic transformation occurs in a single stage from high temperature parent B2 phase to low temperature B19′ monoclinic martensite. After certain thermomechanical treatments, or addition of a third element, the transformation sequence of TiNi SMAs can change into a two-stage B2 to premartensite R-phase to B19′ during cooling [1]. In addition, aged Ni-rich TiNi alloys with scattered Ti$_3$Ni$_4$ precipitates in the matrix can exhibit either B2 ↔ R ↔ B19′ transformation sequence with two distinct steps during both cooling and heating runs, or a B2 → R → B19′ and B19′ → B2 transformation sequence with two distinct steps during cooling and only one step during heating [2].

In the past decade, the martensitic transformation was found to be able to appear in more than two distinct steps and is said to be a multi-stage martensitic transformation (MST). This MST occurring in TiNi alloys has been widely observed using differential scanning calorimetry (DSC), although the cause of this behavior is still controversial. Todoroki and Tamura [3] first explained the effect of cold working on the transformation sequence of TiNi SMAs. Lo et al. [4] also found a two-stage transformation in as-quenched Ti$_{40}$Ni$_{50}$Cu$_{10}$ with B2 → B19 and B19 → B19′ transformations, where B19 is an orthorhombic martensite. Bataillard et al. [5,6] attributed the cause of MST to the stress fields formed around the coherent interfaces between B2 matrix and Ti$_3$Ni$_4$ precipitates, whereas Morawiec et al. [7–9] explained MST to be due to the changes of dislocation configuration by low-temperature annealing. In a recent study, Khalil-Allafi et al. [10] found two distinct steps of B2 → R and R → B19′, and an additional step with B2 → B19′ in the DSC cooling curves of annealed Ni-rich TiNi alloys. They attributed the cause of MST to the Ni-concentration inhomogeneity between Ti$_3$Ni$_4$ precipitates and the difference in nucleation barriers for R-phase and B19′ formations. However, they soon corrected these proposed reasons with the argument that the heterogeneous microstructure between regions with and without Ti$_3$Ni$_4$ precipitates is responsible for the MST behaviors [11]. Recently, Chrobak et al. [12] stated that the MST in the early stage of annealed Ti$_{49.3}$Ni$_{50.7}$ with 10% cold-working had two transformation peaks

* Corresponding author. Tel.: +886-2-2363-7846; fax: +886-2-2363-4562.

E-mail address: skw@ccms.ntu.edu.tw (S.K. Wu).

of $B2 \rightarrow R$ and $R \rightarrow B19'$, and that the $R \rightarrow B19'$ peak consists of two transformation sub-peaks occurring at different temperatures.

According to reports in the literature, a total of three transformation steps have been observed in the DSC cooling curve of TiNi SMAs. In this study, a four-stage MST is found in the deformed and annealed Ni-rich $Ti_{49}Ni_{51}$ SMAs. The transformation sequence of this four-stage MST is discussed to gain a better understanding of the cause and mechanism of MST behaviors.

2. Experimental

The conventional tungsten arc-melting technique was employed to prepare the Ni-rich $Ti_{49}Ni_{51}$ SMA. Titanium (99.7 wt%) and nickel (99.98%), totaling nearly 140 g, were melted and remelted at least six times in an argon atmosphere with pure Ti as the getter. The mass loss during the melting was negligible. The ingot was hot rolled at 850 °C into a plate with 2 mm thickness and then solution-treated at 800 °C for 2 h followed by quenching with water. Thereafter, the solution-treated plate was cold-rolled to obtain 20% thickness reduction and then cut into specimens to conduct DSC, dynamic mechanical analyzer (DMA), and electrical resistivity (ER) tests. The cut specimens were then annealed at 500 °C for various time intervals between 0.5 and 200 h.

The transformation behavior and characteristic temperatures were determined using a DSC cell (TA Q series Q10) with the specimen weight between 40 and 60 mg. In DSC tests, specimens were heated up to 100 °C and kept isothermal for 3 min to obtain thermal equilibrium, then cooled down to −120 °C, and also kept isothermal for 3 min and then brought back to 100 °C again. All heating and cooling rates were kept at 10 °C/min.

The changes of mechanical characteristics during the transformation were observed using DMA (TA 2980 model) in the multi-frequency mode. Specimens with the size of $35 \times 5 \times 1.7$ mm were measured in the same sequence and temperature range as in the DSC test, except that the ramp rate was 3 °C/min. The measuring frequency was 1Hz and the amplitude was 2 μm. The volume of DMA specimen chamber was much larger than that of DSC, and the thermocouple was placed farther from the specimen in DMA than in DSC. As a result, for the same thermomechanical treated specimen, a temperature lag of about 10 °C is observed between DSC and DMA results.

The martensitic and R phase transformation behaviors were also measured using a four-probe ER test in constant current mode. The system for measurement was composed of a temperature control device (Cryocon 32B by Cryogenic Control Systems, Inc.), a power supply (GP0250-3R DC power supply), and a data re-

cording system (Keithley 2000 Multimeter for voltage measurement, and the PCI-GPIB interface card of NI for recording). Specimens with the size of $35 \times 5 \times 1.7$ mm were heated up to 100 °C and then cooled down with a rate of 4 °C/min. Data were recorded from 70 to −50 °C.

3. Results and discussion

3.1. DSC results

DSC results of 20% deformed $Ti_{49}Ni_{51}$ alloy annealed at 500 °C for different time intervals are shown in Figs. 1 and 2. Fig. 1 indicates that the 0.5-h curve remains a typical transformation sequence of aged Ni-rich TiNi SMAs, with two distinct transformation peaks of $B2 \leftrightarrow R$ and $R \leftrightarrow B19'$. After 3 h of annealing, the two reverse transformation peaks merge to become a single peak of $B19' \rightarrow B2$, and later this single peak in the heating curve tends to widen towards high temperature after annealing for 24 h, as indicated by the arrow in Fig. 1. When the specimens were annealed further for 48, 72, 100, and 125 h, the transformation behavior changed and evolved to a four-stage transformation in cooling, as shown in Fig. 2(a). The corresponding heating curves of Fig. 2(a) are shown in Fig. 2(b). In Fig. 2, the arrows 1–4, 1′, and 2′ indicate transformation
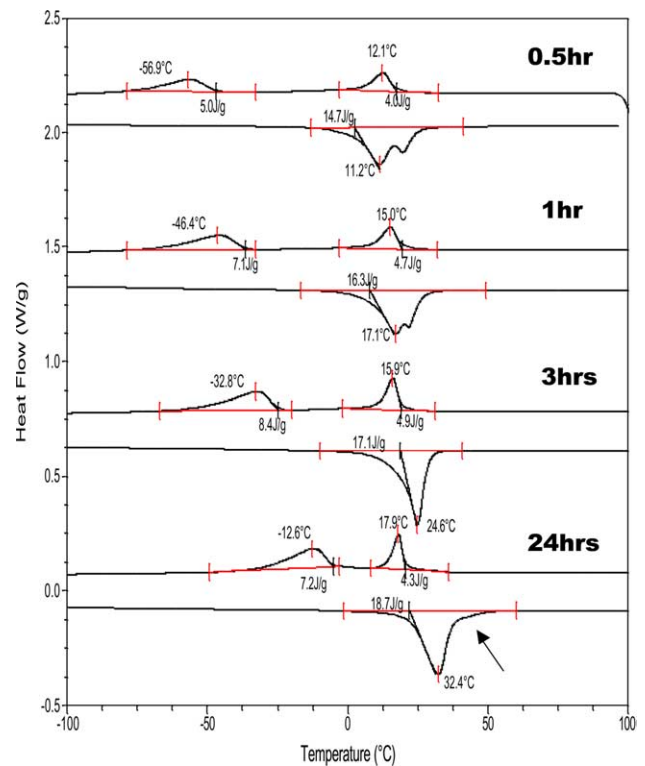

Fig. 1. DSC cooling–heating curves for 20% cold-rolled $Ti_{49}Ni_{51}$ annealed at 500 °C for 0.5, 1, 3 and 24 h.
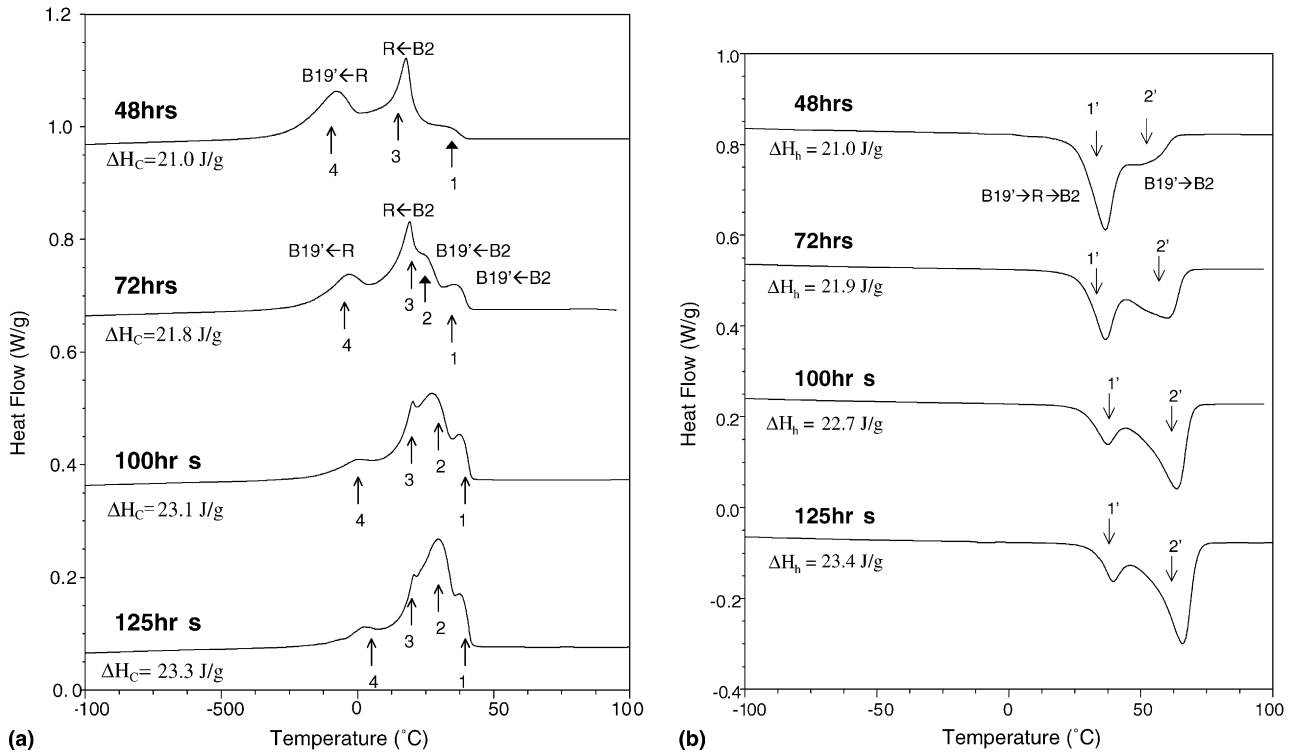
Fig. 2. DSC cooling–heating curves for 20% cold-rolled $Ti_{49}Ni_{51}$ annealed at 500 °C for 48, 72, 100 and 125 h (a) cooling and (b) heating.

peaks 1–4, 1′ and 2′, respectively. In Fig. 2(a) of the 48-h cooling curve, a new transformation peak (peak 1) appears before the original B2 → R peak (peak 3), and it also appears as a new peak after the original B19′ → B2 transformation peak in the corresponding heating curve in Fig. 2(b). After 72 h of aging, another new peak (peak 2) appears between the original B2 → R peak (peak 3) and the peak 1. These results clearly reveal a four-stage transformation behavior (peak 4 is the original R → B19′ peak shown in Fig. 1). When annealed up to 100 and 125 h, the new peaks in cooling (peaks 1 and 2) and in heating (peak 2′) become more prominent than the original peaks (peaks 3, 4 and 1′). Fig. 3(a) and (b) plot the peak temperature and total transformation heat in heating ΔH_h vs. annealing time, respectively, from the data in Figs. 1 and 2.

3.2. DMA results

Fig. 4(a) shows the DMA storage modulus cooling curves of specimens annealed at 48, 72, 100, and 150 h. In the typical DMA curves of TiNi alloys, the storage modulus curve shows a minimum upon transformation, and the B2 → R has a relatively deep minimum compared to that of R → B19′ [2]. These characteristics are also visible in the 48-h curve shown in Fig. 4(a). In the DSC curves of Fig. 2(a), the 48-h annealed specimen already shows a new peak 1, but in Fig. 4(a), no apparent transformation minimum is found. This may be
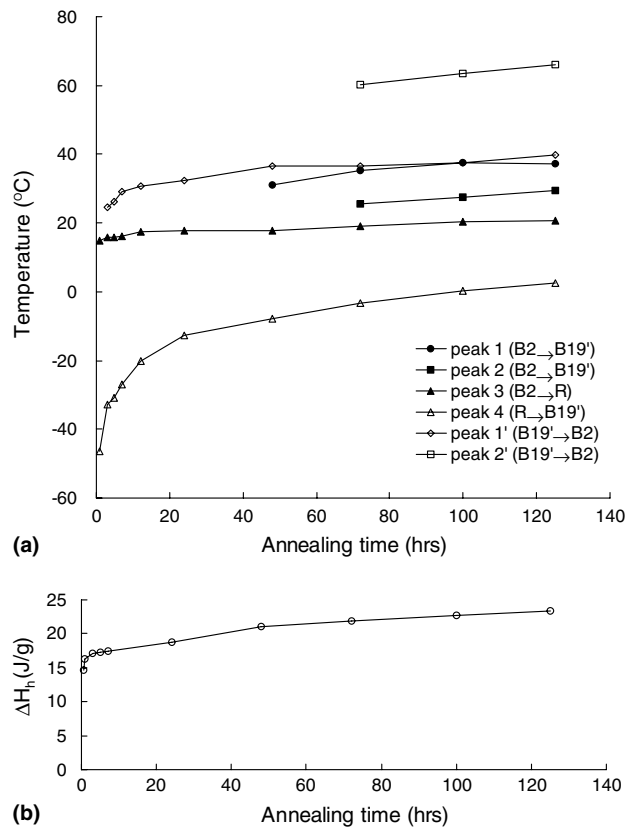

Fig. 3. Transformation temperature and heat evolution of 20% cold-rolled $Ti_{49}Ni_{51}$ annealed at 500 °C.
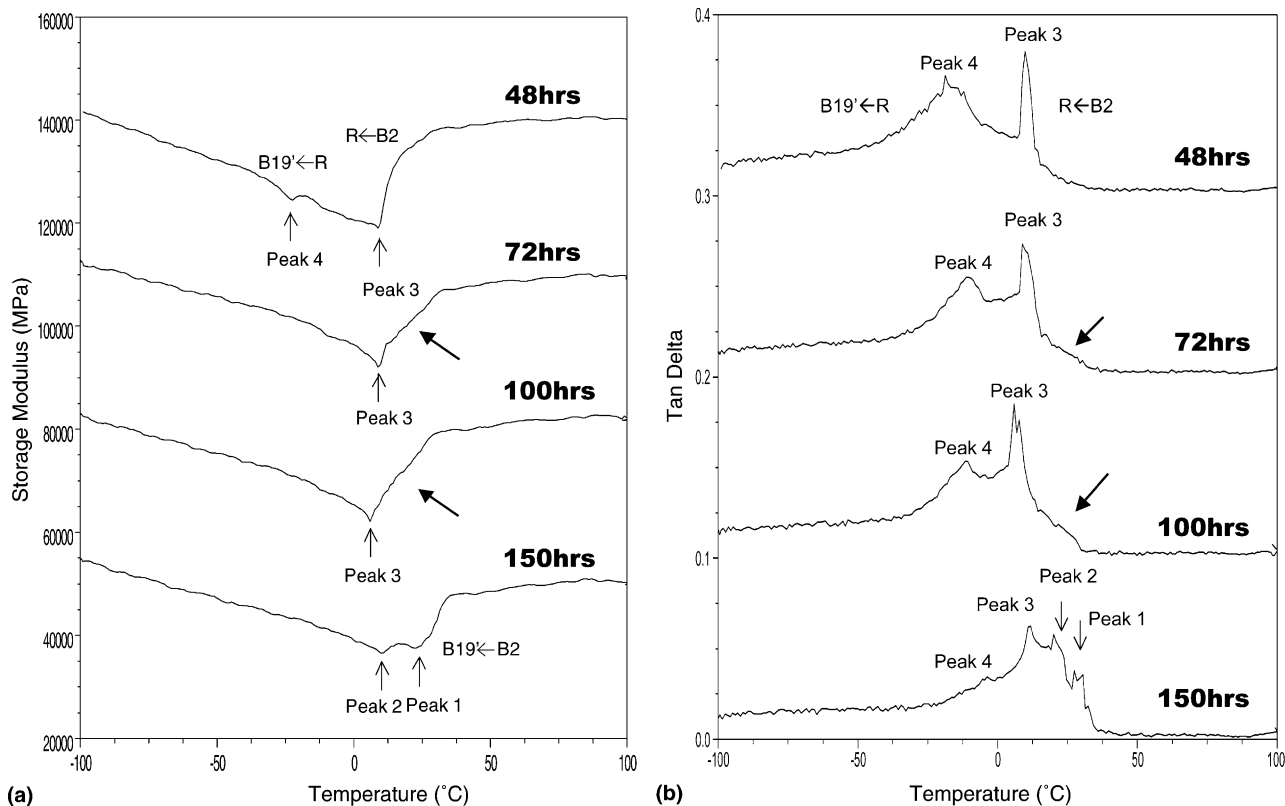
Fig. 4. DMA curves for $Ti_{49}Ni_{51}$ annealed at 500 °C for 48, 72, 100 and 150 h. (a) storage modulus and (b) tan δ.

due to the fact that the transformation volume is not large enough to appear in the DMA results. In the 72 and 100 h curves, the amount of R → B19′ transformation (peak 4) is reduced and thus the minima can no longer be seen, but the B2 → R (peak 3) minima are clearly affected by the newborn peaks 1 and 2 in such a way that the curves go to the minima less abruptly, as indicated by bold arrows in Fig. 4(a). After 150 h of annealing, the peak 3 of B2 → R transformation is almost covered by peak 2 because the relative depth of the minima are smaller compared to the curves obtained at 48–100 h, and thus the two minima in the storage modulus curve should correspond to peaks 1 and 2 individually. The tan delta curves corresponding to Fig. 4(a), which show the damping property changes during transformation, are shown in Fig. 4(b). Typically the tan delta peak corresponding to R-phase transformation is sharper and the transformation is completed within a shorter temperature range, whereas the peak corresponding to martensitic transformation is broader and covers a wider temperature range [2]. In Fig. 4(b), the 48-h curve, no apparent increase in the damping capacity can be found for the appearance of peak 1 for the same reason as stated in the case of Fig. 4(a). At 72 and 100 h, the shoulder before B2 → R transformation peak becomes higher because of the development of peaks 1 and 2, as indicated by the bold arrows in

Fig. 4(b). At 150 h, two distinct peaks corresponding to peaks 1 and 2 are observed.

3.3. ER results

Fig. 5 shows the plots of ER vs. temperature for $Ti_{49}Ni_{51}$ SMAs annealed at 500 °C for 48, 72, and 100 h. In the 48-h curve, the ER does not reflect the existence of peak 1 in DSC curve, and only an abrupt increase in the ER of B2 → R transformation can be observed. However, in the 72 and 100 h curves, before the B2 → R transformation (peak 3), there can be seen the B2 → B19′ martensitic transformation characteristic, which tends to lower the ER value and thus causes the original uprising curve to decrease and even stop increasing, as indicated by bold arrows in Fig. 5. This provides evidence for our viewpoint that peaks 1 and 2 are related to the B2 → B19′ transformation, as discussed further in Section 3.4.

3.4. Discussion of the transformation behavior of four-step MST in cooling

3.4.1. Cause of extra peaks

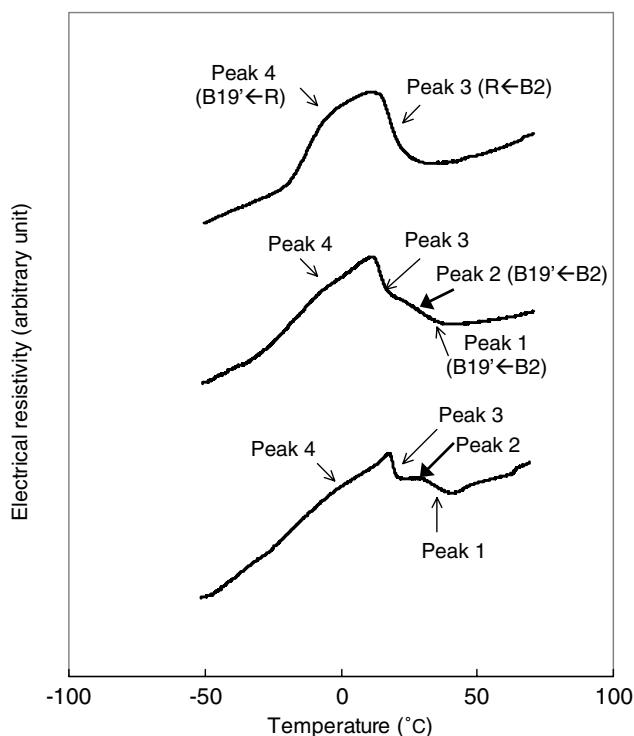In Figs. 1 and 2, the peaks 3, 4, and 1′ correspond to the B2 → R, R → B19′, and B19′ → B2 transformations,

Fig. 5. Electrical resistivity vs. temperature cooling curves for $Ti_{49}Ni_{51}$ annealed at 500 °C for 48, 72, and 100 h.

Fig. 6. Evolution of transformation peak heights for $Ti_{49}Ni_{51}$ annealed at 500 °C for 48, 72, 100, and 125 h.

respectively, similar to those already reported [1,2]. Since we have two new peaks (peaks 1 and 2), instead of only one peak as observed in the past studies, we chemically etched off the 50% thickness from both sides of the rolling surface of the 20% deformed specimen, and performed the DSC test to see if these two extra peaks were caused by non-uniform cold-working reduction between the surface and center areas of the deformed plate. However, the DSC results were the same, thus ruling out the possibility of cold-working non-uniformity to cause the MST in Fig. 2.

Fig. 6 plots the peak height vs. annealing time from the data of Fig. 2. In Fig. 6, the height of peak 3 (B2 → R) does not change significantly when MST appears. Also, its peak temperature remains almost constant, as shown in Fig. 3. The peak temperature of peak 4 (R → B19′) evolves with time in a similar way as the R → B19′ peak in non-deformed $Ti_{49}Ni_{51}$ annealed at 400 °C [13]. Also in Fig. 6, the heights of peaks 4 and 1′ are clearly lower as extra peaks 1, 2 and 2′ appear and grow prominently. This phenomenon indicates that the MST shown in Fig. 2 is closely related to martensitic transformation, instead of R phase transformation. It is well known that the high density of dislocations induced by cold-working in the specimen will suppress its martensitic transformation. In Fig. 1 (the 1-h curve), for example, the transformation heat, ΔH_C, of the two peaks in cooling has a sum of 11.8 J/g, which is smaller than the reverse transformation heat of 16.3 J/g. This
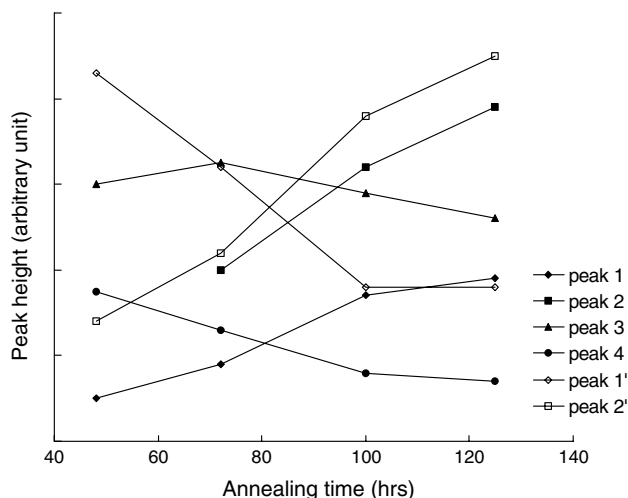
loss of about 5 J/g heat is believed to be covered by the transformation between the two peaks of B2 → R and R → B19′ in cooling. That is, the martensite transforms continuously from R-phase after the appearance of the B2 → R peak. Furthermore, the B19′ → B2 reverse transformation heat (16.3 J/g) is much smaller than that of TiNi specimens which have not undergone cold work, which is about 25 J/g [14]. Therefore, there should be a large amount of martensitic transformation which is hindered by the high density of dislocations induced by cold-rolling. Fig. 3(b) shows the ΔH_h evolution curve in the reverse transformation of Figs. 1 and 2. In Fig. 3, the ΔH_h has an apparent increase as the MST appears after 24 h of annealing; and it is as large as 23.4 J/g at 125 h of annealing, reaching about 25 J/g at 200 h of annealing (not shown in Fig. 2). These phenomena indicate that the originally suppressed martensitic transformation is released after being annealed for a long period of time, re-appearing and producing new peaks 1, 2, and 2′ instead of merely increasing the ΔH of the existing peaks, 3, 4, and 1′.

3.4.2. The transformation behavior of the extra peaks

The reported MST of Ni-rich TiNi alloy during cooling consists of a B2 → R peak, an R → B19′ peak, and an extra peak that appears after the B2 → R peak [8,10–12]. However, in this study, except for the B2 → R and R → B19′ peaks, two extra peaks (peaks 1 and 2) shown in Fig. 2 are observed before the B2 → R peak but not after the B2 → R peak. The reason that the two extra peaks observed in the present case appear before the B2 → R peak may be due to the long-term annealing of Ni-rich TiNi specimens and thus the Ti_3Ni_4 precipitating effect makes the composition of the matrix between precipitates reach near equiatomic TiNi. Thus, the B2 matrix has a transformation

temperature (peaks 1 and 2 of Figs. 2 and 3) above room temperature during cooling. We suggest that peaks 1 and 2 in Fig. 2(a) should be two separate $B2 \rightarrow B19'$ transformations, both corresponding to peak $2'$ of Fig. 2(b).

Recently, Chrobak et al. [12] deformed $Ti_{49.3}Ni_{50.7}$ SMA with 10% reduction and annealed in a much shorter time (5–240 min) and to a lower temperature (400 °C) than we did. From their TEM observations, the Ti_3Ni_4 precipitates would decorate the dislocations induced by cold-working. The dislocations in some precipitate free areas are bowed after 240 min of annealing and hence the deformed sample stores less elastic energy. Chrobak et al. [12] suggested that the sample volume is divided into areas that differ in the density of precipitates,so two separate $R \rightarrow B19'$ peaks occur. Khalil-Allafi et al. [11] also attributed the cause of MST in non-deformed $Ti_{49.4}Ni_{50.6}$ SMA to the same reason, but their three-step transformation peaks are $B2 \rightarrow R$ and $R \rightarrow B19'$, both of which transform in regions with precipitate; and the other $B2 \rightarrow B19'$ peak occurs in precipitates free regions. In the present study, we suggest that our two extra steps of $B2 \rightarrow B19'$ (peaks 1 and 2 of Fig. 2) can also be caused by the difference of the required martensitic transformation energy between different sample areas. The larger cold-working reduction induces relatively higher dislocation density, and these dislocations will recover around the precipitates upon increasing the annealing time. According to the argument of [12], we suggest that the volume with higher precipitate density in our long-time annealed sample will accumulate higher dislocation density where more energy is needed to start martensitic transformation. On the other hand, the precipitate free volume in the sample will have low dislocation density and thus needs less energy to transform the martensite. As the annealing time increases, the dislocations bend more toward the precipitates, resulting in an increase in the high dislocation volume and causing peak 2 to become more prominent. The volume with low dislocation density also increases upon increasing the annealing time due to dislocation recovery in areas between precipitates, and causes peak 1 to grow higher. From Fig. 6, the peak heights of peaks 1 and 2 increase in the same way, but the relative height of peak 2 is much higher than that of peak 1. This may indicate that the volume with high dislocation density is larger than that with low dislocation density.

4. Conclusion

The two extra steps during the forward transformation can be interpreted as follows. Peak 1 corresponds to the $B2 \rightarrow B19'$ transformation in the low dislocation density region, and peak 2 also corresponds to the $B2 \rightarrow B19'$ transformation but now in the high dislocation density region. These peaks are not related to R phase transformation. The one extra step in the reverse transformation corresponds to peaks 1 and 2 and is a $B19' \rightarrow B2$ transformation. These two extra transformation peaks occurring in cooling are related to the reappearance of martensitic transformation that is suppressed by dislocations induced by cold-working. The extra peaks may appear before $B2 \rightarrow R$ transformation peak due to the higher temperature and longer annealing time applied in this study,which make the composition of matrix very close to equiatomic TiNi SMA. The four-step process of transformation behavior observed in this study, which is even more complex than the results of past studies, is suggested to be the result of combined effect of severe cold-working and long-time annealing, and is not caused by the cold-working non-uniformity between the surface and center areas of the deformed plate.

References

[1] Funakubo H. Shape memory alloys. OPA Amsterdam: Gordon and Breach Science Publishers; 1987. p. 63.
[2] Wu SK, Lin HC, Chou TS. Acta Metall Mater 1990;38:95.
[3] Todoroki T, Tamura H. Trans Jpn Inst Met 1987;28:83.
[4] Lo YC, Wu SK, Horng HE. Acta Met Mater 1993;41:747.
[5] Bataillard L, Gotthardt R. J de Phys III 1995;5:C8–647.
[6] Bataillard L, Bidaux J-E, Gotthardt R. Philos Mag 1998;78:327.
[7] Morawiec H, Stróz D, Chrobak D. J de Phys IV 1995;5:C2–155.
[8] Morawiec H, Stróz D, Goryczka T, Chrobak D. Scr Mater 1996;35:485.
[9] Morawiec H, Ilczukl J, Stróz D, Goryczka T, Chrobak D. J de Phys IV 1997;7:C5–C155.
[10] Khalil-Allafi J, Ren X, Eggeler G. Acta Mater 2002;50:793.
[11] Khalil-Allafi J, Dlouhy A, Eggeler G. Acta Mater 2002;50:4255.
[12] Chrobak D, Stróz D, Morawiec H. Scr Mater 2003;48:571.
[13] Lin HC, Wu SK. Scr Metall Mater 1991;25:1529.
[14] Goo E, Sinclair R. Acta Metall Mater 1985;33:1717.